
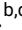

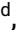






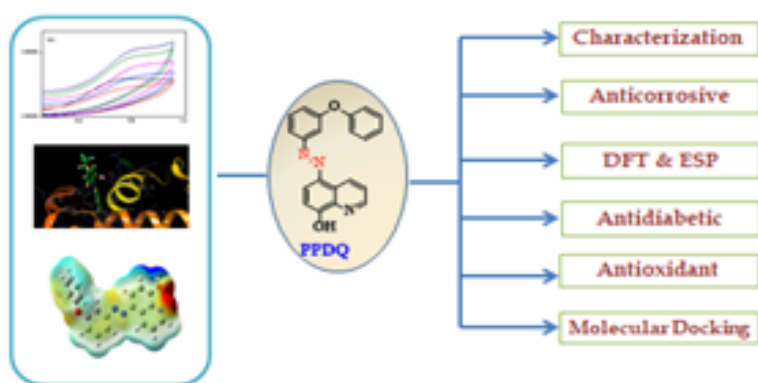
Full Paper | <http://dx.doi.org/10.17807/orbital.v16i3.21006>

E5-((3-phenoxyphenyl)diazenyl)quinolin-8-ol (PPDQ) : A Novel Promising Anticorrosive for Mild Steel in Acid Media, and a Pharmacologically Potent Antidiabetic, Antioxidant Azo Dye

Pruthviraj K. ^a, Chethan B. S. ^{b,d}, Ramesha H. ^c, Lokanath N. K. ^d, Kiran P. C. ^c, Devaraju K. S. ^c, Narayana Hebbar N. ^{e*}, and Sunil K. ^{a**}

A novel quinoline based azo dye 5-((3-phenoxyphenyl)diazenyl)quinolin-8-ol (PPDQ) was synthesized using conventional one pot MCR pathway and its structure has been confirmed by multinuclear (¹H & ¹³C) and mass spectral techniques. PPDQ subjected for remarkable analytical applications like anticorrosion potential for mild steel in acidic media. Further, the experimental results were compared with that of the theoretical DFT based calculations and found to be in good agreement with each other. To evaluate the pharmacological activity of the compound *in vitro* antidiabetic and antioxidant activity were carried out. The corrosion inhibition potential of the PPDQ was explored using electrochemical method which exhibited maximum corrosion inhibition efficiency up to 77% on mild steel in 1 M HCl media, further the anticorrosion potential was confirmed by quantum chemical calculations (DFT, ESP diagrams). Antidiabetic activity and antioxidant potency was evaluated using DPPH, and ABTS radical scavenging assay. Further, the *in-vitro* values were compared with *insilico* molecular docking studies.

Graphical abstract



Keywords

PPDQ
Anticorrosion potential
DFT
Anti-diabetic
Antioxidant activity
Molecular docking

Article history

Received 27 Apr 2024
Revised 31 Jul 2024
Accepted 18 Sept 2024
Available online 17 Oct 2024

Handling Editor: Adilson Beatriz

1. Introduction

^a Department of Chemistry, Sri Siddhartha Institute of Technology, SSAHE, Tumakuru – 572105. ^b Department of Basic Science, Amruta Institute of Engineering and Management Sciences, Bidadi, Bengaluru-572109. ^c Neuro-chemistry Lab, Department of Biochemistry, Karnatak University, Dharwad-580003. ^d Department of Studies in Physics, Manasagangotri, University of Mysore, Mysuru – 570006. ^e Department of PG studies and Research in Chemistry, Sri Dharmasthala Manjunatheshwara College (Autonomous), Ujire-574240. Corresponding author. E-mail: sunilk999@gmail.com; dr.nahebbar@sdmcyjire.in

Low carbon steel, or mild steel, has a carbon content of only 0.05–0.25%, with an additional prevalent alloying element manganese [1], which finds extensive application in diverse fields such as automotive, construction, machinery building, and other domains, is easily susceptible to corrosion in acid media [2]. Chemical laboratories and various industrial processes, including oil wet cleaning, acid pickling, acid cleaning, and descaling, use a lot of acidic solutions [3]. One of the most practical ways to prevent metallic corrosion is to use inhibitors, particularly in acidic media [4]. The affordability, substrate material inhibition efficacy, and environmental side effects of an inhibitor all play a role in the choice of inhibitor. Hence, organic compounds make up the majority of the best acid inhibitors for preventing steel from corroding in acidic media [5]. Compounds with polar functional groups, heteroatoms such as N, O, S, and P either in the side chain or in the ring, and delocalized π electrons. These features serve as adsorption sites, enabling molecules to be adsorbed on the metal surface and creating a barrier that lessens the damaging effects of the acidic solution on the metal [6–8]. The interaction of compounds with π -bonds with the d-orbital on the metal surface results in good inhibitory characteristics in general. Each of the aforementioned traits is combined with a structure that renders the azomethine and azo dye compounds, which contain $-C=N-$ and $-N=N-$ bond linking respectively as potential corrosion inhibitors [9–13]. One of the most significant, diverse, and expansive classes of organic compounds are azo dyes, which find application in a number of fields such as anticorrosion, fabric dyeing, organic solar cells, OLEDs, and more [14–16]. Regarding their pharmacological potency, azo dyes fall into the categories of antibacterial [17], antidiabetic [18], anticancer [19] and antioxidant agents [20], which are recognized for their ability to act as lipid peroxidation retardants, can minimize the health risks associated with ROS, RNS, and lipid peroxidation by acting as antioxidant agents in the food and drug industries. They can also reduce or limit the effects of oxidative damage in biological tissue structures by scavenging free radicals [21–23].

In the current study, a quinoline bearing a novel azo dye as a corrosion inhibitor and a potent antioxidant, E5-((3-phenoxyphenyl) diazenyl) quinolin-8-ol (PPDQ), was prepared. Its anticorrosive potency in 1M HCl media and its potent antioxidant activity were examined using invitro DPPH, ABTS, and H_2O_2 free radical scavenging assay method. Comparatively, a compound's efficiency is determined by its chemical makeup and structure. The data were confirmed through quantum chemical calculations such as DFT and ESP. Additionally, the in vitro antioxidant assay was supported by molecular docking analysis and electrochemical voltammogram studies.

2. Material and Methods

Analytical grade chemicals and reagents were acquired from Spectrochem and Sigma Aldrich. Melting points (m.p) of the compound determined using open capillary tubes and are uncorrected. Reactions were monitored by Thin Layer Chromatography (60 F254) aluminum sheets and visualization was done by UV light. 1H NMR and ^{13}C NMR spectra was recorded on ECX500 Jeol 400 MHz high resolution multinuclear FT NMR Spectrometer with LN_2 cooled probe with internal TMS and chemical shifts were expressed in parts per million (ppm) using $DMSO-d_6$ as solvent. HRMS was recorded on Maxis Impact (BRUKER)

high detection mass spectrometry with ESI +ve and -ve mode.

Corrosion Inhibition

The commercially procured low carbon steel strips with the elemental composition of 0.05 % C, 0.32 % Mn, 0.019 % P, 0.041 % S, and the 99. 57 % Fe was used for all the corrosion experiments. a 1 cm^2 exposed section of steel strip has been utilised, with the remaining surface covered by epoxy resin insulation. Sand paper with silicon carbide was used to abrade all of the steel strips that were utilised for the measurements. The strips were then cleaned with deionized water after being degreased with acetone. PPDQ, also known as E5-((3-phenoxyphenyl) diazenyl)quinolin-8-ol, was dissolved in 1M HCl, a corrosive medium. These made inhibited solutions at various concentrations, examined using electrochemical techniques, have been employed in all corrosion investigations. The Tafel polarisation method and the AC impedance method are electrochemical methods that are carried out using an Electrochemical Workstation (CH instrument). The values obtained from the software of the CHI 660E electrochemical work station (made by CH Instruments, Austin, USA) at 303 K are reported, and Zsimp Win software is used to fit the circuit for the AC impedance plots [24–26]

In-vitro anti-diabetic activity

Alpha amylase inhibition assay; The α -amylase inhibitory activity of synthesized PPDQ samples was performed according to the method developed by Vishnupriyan Varadharaj *et al.* [27]. using 3, 5-dinitrosalicylic acid reagent. 0.2 mL of PPDQ sample at different concentration (50 μg to 250 μg) in DMSO was incubated with 0.2 mL of α -amylase (2 units / ml) were incubated for 10 min at 37°C. Furthermore 1 % of soluble starch (0.2 ml) was added and incubated for 5 min at 37°C. the mixture was boiled for 10 min at 90 °C than cooled the reaction mixture and add 1.5 ml of distilled water, finally the absorbance was measurement at 540 nm using UV-Vis spectrophotometer (UV-1800 Shimadzu). Experiments were triplicate and plotted the graph ageist the control (standard control used as acarbose) and The α -amylase inhibitory activity was calculated as percentage (%) inhibition, based on followed equation.

$$\% \text{ Inhibition} = [(A_{\text{control}} - A_{\text{blank}}) - (A_{\text{sample}} - A_{\text{blank}})] / (A_{\text{control}} - A_{\text{blank}}) \times 100$$

In-vitro antioxidant activity

DPPH activity; The antioxidant activity of the synthesized PPDQ samples was determined using the DPPH free radical assay described by Badiger K B *et al.* [28]. and Hanumegowda S *et al.* [29]. with some modifications. The synthesized PPDQ samples were dissolved in DMSO (1 $\mu g/\mu l$), and different concentration from 50 μg to 250 μg in different tubes compose volume 860 μl of 50% methanol and finally 140 μl of DDPH was added. The resulting mixture was agitated and incubated for 30 minutes at room temperature in a dark place and was then read by a UV-Vis spectrophotometer (UV-1800 Shimadzu) at 512 nm. Experiments were triplicate and plotted the graph against the control. Ascorbic acid (AC) was used as a control scavenging effect and was calculated using the following equation.

$$= \frac{\text{Absorbance of control} - \text{absorbance of sample}}{\text{Absorbance of control}} \times 100$$

In-vitro ABTS activity

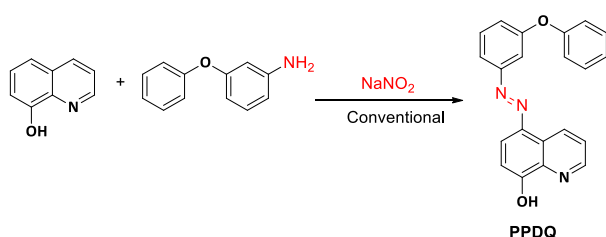
Estimation of radical scavenging activity of synthesized PPDQ was carried out using the method described by Maarif Khan *et al.* [30], Different concentrations of PPDQ and ascorbic acid (50 to 250 µg/ml), and 1 ml of ABTS⁺ in Potassium persulfate mixture were incubated for 30 min in a dark place. Finally, a slightly formed yellow coloured reaction was observed at 734 nm. The scavenging percentage of PPDQ was calculated using the following formula.

$$= \frac{\text{Absorbance of control} - \text{absorbance of sample}}{\text{Absorbance of control}} \times 100$$

3. Results and Discussion

Synthesis and Characterization of E5-((3-phenoxyphenyl)diazenyl)quinolin-8-ol (PPDQ)

The title compound was prepared using normal diazot coupling reaction as reported, thus obtained compound was characterized using various spectral techniques (Scheme 1).



Scheme 1. Synthesis of PPDQ. ¹H NMR (400MHz, DMSO-d₆, δ, ppm): 5.351 (b, 1H, Ar-OH), 6.901-7.381 (m, 6H, ArH), 7.470-8.120 (m, 6H, ArH), 8.21 (d,1H, ArH), 8.58 (d,1H, ArH), ¹³C NMR (100MHz, DMSO-d₆, δ, ppm): 112.8, 109.4, 116.7-116.8 (3C), 116.7, 117.7, 121.1, 122.2, 122.4, 127.8, 129.4, 129.7, 131.7, 136.7, 146.8, 147.3, 149.8, 153.4, 156.3, 160.1. MS: Calculated= 341.11 Observed- (M+1)= 342.1.

Evaluation of Corrosion Inhibition Potency

Tafel Polarization measurements

The absolute corrosion rate can measure by the electrochemical technique of polarization resistance and it expressed in Milli-inches per year (mpy). Polarization resistance also called as "linear polarization". The obtained Tafel plots are as shown in Figure 1. The electrochemical corrosion kinetic parameters such as corrosion potential (E_{corr}), corrosion current density (i_{corr}) and inhibition efficiency (η_p) are reported in Table 1.

A potentiodynamic polarization plot, such can yield important information such as The Tafel extrapolation method is very accurate which is equal or greater than conventional weight loss methods. It is possible to measure extremely low corrosion rates by using potentiodynamic polarization plots. Tafel plots can provide a direct measure of the corrosion current [31]. As expected, As the increase in the concentration of inhibitor, the rate of corrosion was inhibited. The addition of the inhibitor that reduces the

anodic reaction and also retards the cathodic reaction. According to literature the compound can be classified as an anodic or cathodic inhibitor when the potential displacement is at least 85 mV with respect to the blank solution.

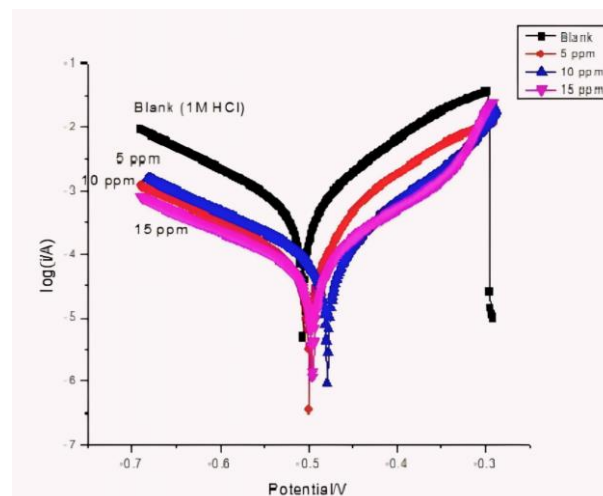


Fig. 1. Tafel plots for steel in the absence and presence of different concentrations of PPDQ in 1 M HCl at a 303 K.

Table 1. Electrochemical Tafel polarization parameters for steel in the absence and presence of various concentrations of PPDQ in 1 M HCl at a temperature 303K

Inhibitor conc. (ppm)	E_{corr} (V)	i_{corr} (mA cm ⁻²)	Corrosion Rate (mpy)	IE (%)
0.1M HCl	-0.492	10.0	1.903	-
5	-0.482	6.5	1.715	35
15	-0.499	5.4	1.404	46
25	-0.497	2.3	1.325	77

AC impedance method

AC impedance Nyquist plots for mild steel in the presence and absence of inhibitor at a different temperature as shown in Figure 2. An equivalent circuit model Figure 3 was used to fit the Nyquist plots [32]. The parameters such as polarization resistance (R_p) and double capacitance values (C_{dl}) are measured using equivalent circuit are listed in Table 2. The depressed semicircle shows the characteristics of solid electrodes Figure 4, and it referred to as frequency dispersion. This frequency dispersion attributed to roughness and inhomogeneities. According to literature, two models have been adopted to describe the EIS spectra for the inhomogeneous films on the metal surface of rough and porous electrodes. One is the filmed equivalent circuit model, and the other is the finite transmission line model. In this work, the filmed equivalent circuit model is used to describe the inhibitor-covered metal/solution/interface. Figure 4 shows the exact agreement between the obtained AC impedance curve and circuit fitment curve [32, 33].

Table 2. AC impedance results.

Inhibitor conc. (ppm)	R_p (Ω cm ²)	C_{dl} (μ F cm ⁻²)	IE (%)
0.1M HCl	47	16.3	-
5	147	12.3	68
15	187	10.4	74
25	223	9.5	78

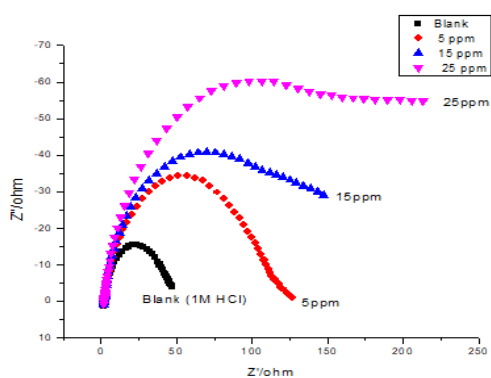


Fig. 2. Nyquist plots for steel in 1 M HCl in the absence and presence of different concentrations of PPDQ at a 303.

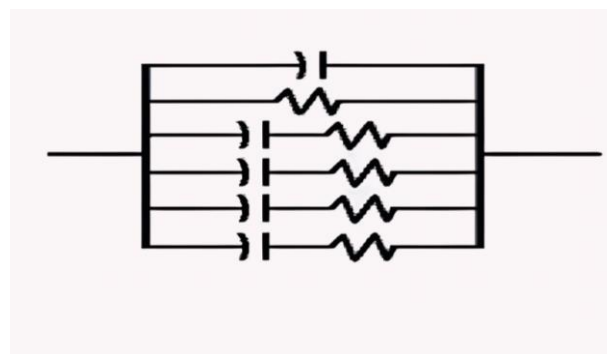


Fig. 3. Circuit for AC impedance plot.

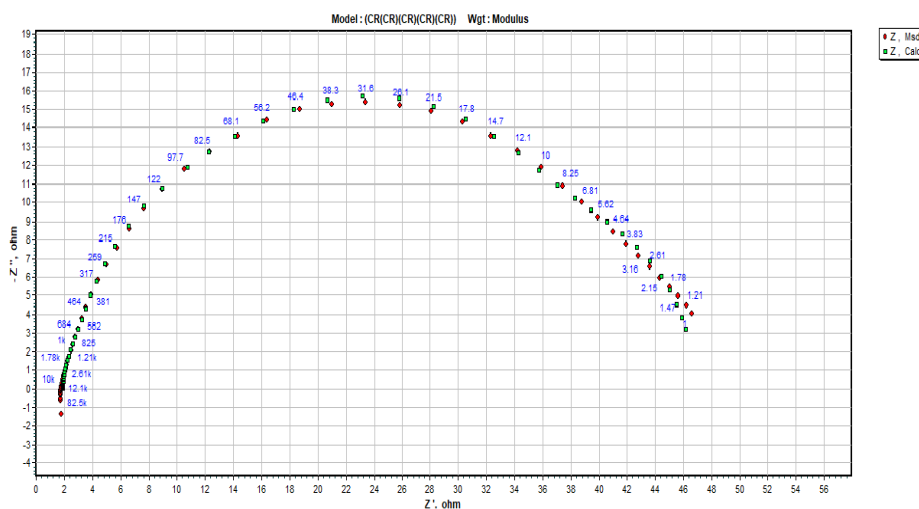


Fig. 4. Nquist plot and plot after applying the circuit.

The experimental results were corroborated using density functional theory studies. The synthesis compound was optimized using B3LYP functional with 6-311G(d,p) basis set. Further, using the optimized structure the electronic properties related to the structure such as E_{HOMO} , E_{LUMO} associated with the electron donating and electron accepting ability of the molecule were evaluated.

The ability of the absorption of the inhibitor to the metal surface increases with increase in the E_{HOMO} and decrease in the E_{LUMO} energies. Further, the HOMO-LUMO energy gap (ΔE) indicates the reactivity of the inhibitor molecule towards the adsorption on the metal surface. The decrease in the ΔE leads to the better inhibition effectiveness. The calculated values of E_{HOMO} , E_{LUMO} and ΔE of the compound under study were evaluated both in gas and aqueous phase and are tabulated in the Table 3.

The effectiveness of these azo inhibitors was mainly confirmed by the electrons on HOMO because when they adsorbed on a metallic surface, the inhibitor could provide electrons to the d-orbital of metal and then form a

coordination bond. The inhibition effectiveness will be higher with increasing E_{HOMO} . The order of HOMO is effectively related to experimental inhibition effectiveness. The frontier molecular orbital distribution of the HOMO and LUMO are provided in the Figure 5 and the distribution of the charges on the molecule is provided in the Figure 6. The HOMO are found to be distributed over the naphthalene group, whereas the LUMO are distributed over N=N group.

The dipole moment μ is an important parameter that measures the polarity of a covalent bond. The high value of the dipole moment likely increases the adsorption between the inhibitor and the metal surface. The energy of the deformability increases with an increase in the μ , making easier adsorption of the molecule at the metal surface indication good corrosion inhibition. The molecular electrostatic potential map revealed the charge distribution on the synthesized molecule and the red and blue colours indicate the electrophilic and nucleophilic regions respectively (Figure 6).

Table 3: Physicochemical Parameters of PPDQ.

E_{HOMO} (eV)	E_{LUMO} (eV)	E_g (eV)	I (eV)	A (eV)	X (eV)	μ (eV)	η (eV)	s (eV ⁻¹)	ω (eV)
-6.0145	-2.7220	3.2926	6.0145	2.7220	4.3682	-4.3682	1.6463	0.6074	5.7953

I : Ionisation energy, A : Electron affinity, X : Electron affinity, μ : Chemical potential, η : Chemical hardness, s : Chemical softness, and ω : Electrophilicity.

compared to ascorbic acid with the IC_{50} value of 43 $\mu\text{g/mL}$ (Figure 8).

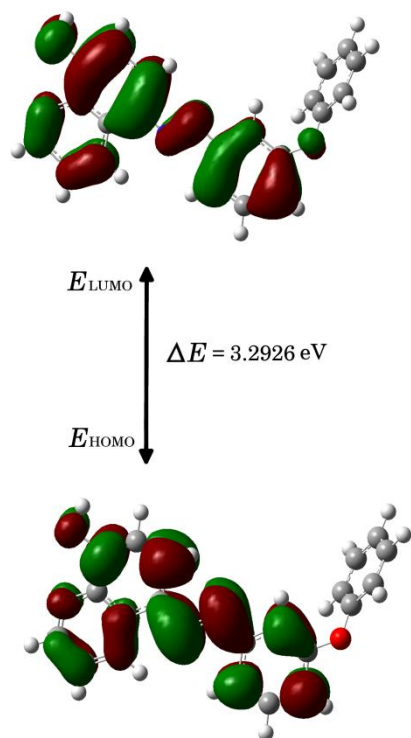


Fig. 5. Distribution of the highest occupied and lowest unoccupied molecular orbitals of the synthesized compound PPDQ.

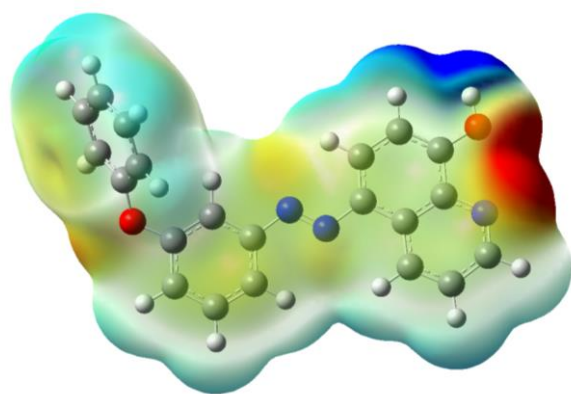


Fig. 6. The molecular electrostatic potential map of the compound revealing the charge distribution.

In-vitro and *In-silico* α -amylase inhibitory assay & *in-vitro* antioxidant activity

From the *in-vitro* data obtained it's found to be PPDQ is showing moderate α -amylase inhibitory activity in comparison with the standard resveratrol drug as showing in bar chart Figure 7a and from the *in-silico* molecular docking studies the binding energy is found to be -3.079 KJ/mol (Figure 7b) on docking with human pancreatic amylase enzyme (PDBID: 6OCN) using Schrodinger which is in agreement with the *in-vitro* value, from the *in-vitro* antioxidant assay as represent below further revealed that PPDQ can be a potent antioxidant agent in comparison with ascorbic acid as shown in PPDQ found to be moderant antioxidant agent

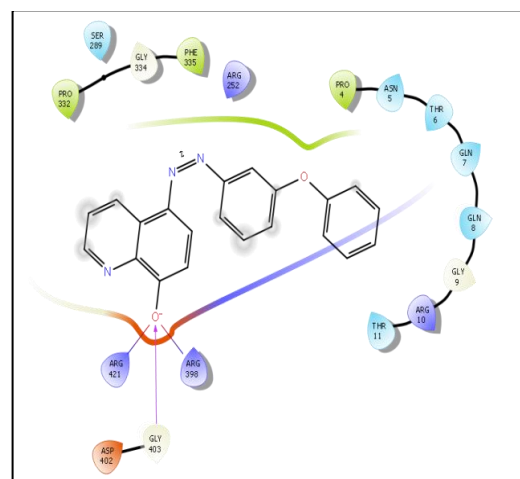
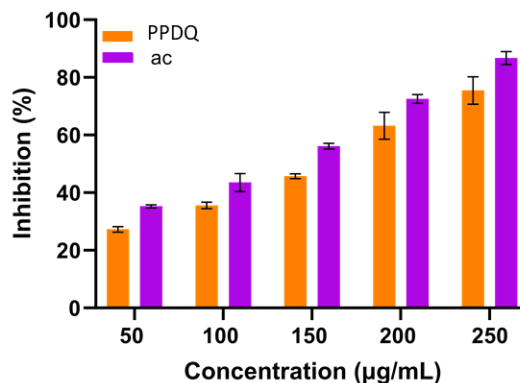


Fig. 7. a) invitro α -amylase activity b) 2D binding mode of interaction.

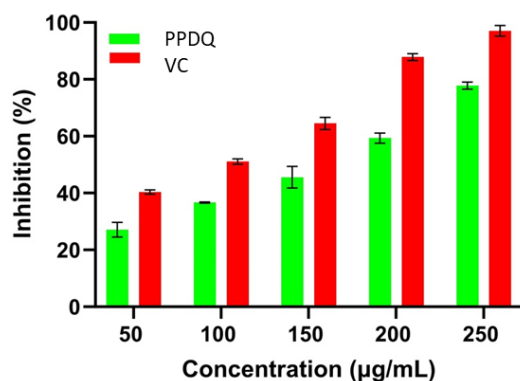
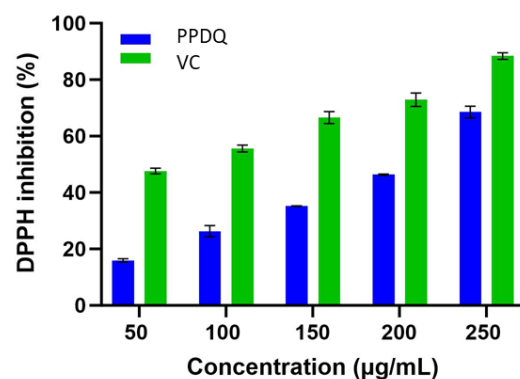


Fig. 8. *In-vitro* antioxidant assay of PPDQ against a) ABTS b) DPPH.

4. Conclusions

A novel quinoline based azo dye 5-((3-phenoxyphenyl)diazenyl)quinolin-8-ol (PPDQ) was synthesized using eco-friendly one pot MCR pathway and its structure has been confirmed by multinuclear (^1H & ^{13}C) and mass spectral techniques. PPDQ subjected for remarkable analytical applications like anticorrosion potential for mild steel in acidic media, antioxidant activity and antidiabetic activity. The corrosion inhibition potential of the PPDQ was explored using electrochemical method which exhibited maximum corrosion inhibition efficiency up to 77% on mild steel in 1M HCl, further the anticorrosion potential was confirmed by quantum chemical calculations (DFT, ESP diagrams). Antidiabetic through α -amylase inhibitory method & antioxidant potency was evaluated using DPPH and ABTS assay, obtained *invitro* values were compared with *insilico* molecular docking result and are in good agreement.

Acknowledgments

Sri Siddhartha Institute of Technology, SSAHE, Tumakuru for providing opportunity to carryout research work and SDM ujire for the collaborative work for the studies of corrosion inhibition.

Author Contributions

Pruthviraj K: Writing Original draft, Methodology, Investigation. Chethan B. S.: Data curation, Validation, Formal analysis. Ramesha H.: Data curation, Validation, Formal analysis. Lokanath N. K.: Methodolgy, Formal analysis, Software. Kiran P. C.: Methodology, Formal analysis. Devaraju K. S.: Resources, Visualization. Narayana Hebbar N.: Resources, Software, Writing-review & editing. Sunil K.: Resources, Project Administration, Writing-review & editing. Supervision

References

- [1] Merwin, M. *Mater. Sci. Forum.* **2007**, 539, 4327. [\[Crossref\]](#)
- [2] Aslam, R.; Mobin, M.; Zehra, S.; Aslam, J. *J. Mol. Liq.* **2022**, 364, 119992. [\[Crossref\]](#)
- [3] Prabhu, R. A.; Venkatesha, T. V.; Shanbhag, A.; Praveen, B. M.; Kulkarni, G. M.; Kalkhambkar, R. G. *Mater. Chem. Phys.* **2008**, 108, 283. [\[Crossref\]](#)
- [4] Chigondo, M.; Chigondo, F. *J. Chem.* **2016**, 1. [\[Crossref\]](#)
- [5] Al-Amiery, A.; Wan Isahak, W.N.R.; Al-Azzawi, W.K. *Ain Shams Eng. J.* **2024**, 15, 102672. [\[Crossref\]](#)
- [6] Desai, P. D.; Pawar, C. B.; Avhad, M. S.; More, A. P. *Vietnam J. Chem.* **2023**, 61, 15. [\[Crossref\]](#)
- [7] Verma, C.; Chauhan, D. S.; Aslam, R.; Banerjee, P.; Aslam, J.; Quadri, T. W.; Zehra, S.; Verma, D. K.; Quraishi, M. A.; Dubey, S.; Al Fantazi, A.; Rasheed, T. *Green Chem.* **2024**, 26, 4270. [\[Crossref\]](#)
- [8] Wang, L.; An, J.; Wang, J.; Gu, J.; Sun, X. *Adv. Colloid Interface Sci.* **2023**, 320, 103031. [\[Crossref\]](#)
- [9] Chen, L.; Lu, D.; Zhang, Y. *Materials* **2022**, 15. [\[Crossref\]](#)
- [10] El-Haddad, M. N.; Fouda, A. S. *Chem. Eng. Commun.* **2013**, 200, 1366. [\[Crossref\]](#)
- [11] Fouda, A. S.; El-Azaly, A. H.; Awad, R. S.; Ahmed, A. M. *Int. J. Electrochem. Sci.* **2014**, 9, 1117. [\[Crossref\]](#)
- [12] Yusoff, M. H.; Azmi, M. N.; Hussin, M. H.; Osman, H.; Raja, P. B.; Rahim, A. A.; Awang, K. *Int. J. Electrochem. Sci.* **2020**, 15, 11742. [\[Crossref\]](#)
- [13] Zobeidi, A.; Neghmouche Nacer, S.; Atia, S.; Kribaa, L.; Kerassa, A.; Kamarchou, A.; AlNoaimi, M.; Ghernaout, D.; Ali, M. A.; Lagum, A. A.; Elboughdiri, N. *ACS Omega* **2023**, 8, 21571. [\[Crossref\]](#)
- [14] Benkhaya, S.; M'rabet, S.; El Harfi, A. **2020**, 6, e03271. [\[Crossref\]](#)
- [15] Eltaboni, F.; Bader, N.; ElKailany, R.; Elsharif, N.; Ahmida, A. *J. Chem. Rev.* **2022**, 4, 313. [\[Crossref\]](#)
- [16] Md. Khan, N.; Parmar, D. K.; Das, D. *Mini-Rev. Med. Chem.* **2021**, 21, 1071. [\[Crossref\]](#)
- [17] Abdel Zaher, K. S.; Shaban, E.; Nawwar, G. A. M. *Chemistry Select.* **2023**, 8, e202300804. [\[Crossref\]](#)
- [18] Tahir, T.; Shahzad, M. L.; Tabassum, R.; Rafiq, R.; Ashfaq, M.; Hassan, M.; Kotwica-Mojzycz, K.; Mojzycz, M. *J. Enzyme Inhib. Med. Chem.* **2021**, 30, 1508. [\[Crossref\]](#)
- [19] Sevastre, A. S.; Baloi, C.; Alexandru, O.; Tataranu, L. G.; Popescu, O. S.; Dricu, A. *Saudi J. Biol. Sci.* **2023**, 30, 103599. [\[Crossref\]](#)
- [20] Muhammad-Ali, M. A.; Hamza, H.; Salman Jasim, E. *Asian J. Pharm. Clin. Res.* **2019**, 479. [\[Crossref\]](#)
- [21] Ashmawy, A.; Alahl, A.; Ali, A. A.; Mahmoud, A.; Rizk, S. *Egypt. J. Chem.* **2022**, 8, 531. [\[Crossref\]](#)
- [22] Jha, P.; Modi, N.; Jobby, R.; Desai, N. L. *Int. J. Phytoremediation.* **2015**, 17, 305. [\[Crossref\]](#)
- [23] Mezgebe, K.; Mulugeta, E. *RSC Adv.* **2022**, 12, 25932. [\[Crossref\]](#)
- [24] Hebbar, N.; Praveen, B. M.; Prasanna, B. M.; Venkatesha, T. V.; Abd Hamid, S. B. *J. Adhes. Sci. Technol.* **2015**, 29, 2692. [\[Crossref\]](#)
- [25] Hebbar, N.; Praveen, B. M.; Prasanna, B. M.; Venkatesha, T. V. *Int. J. Ind. Chem.* **2015**, 6, 221. [\[Crossref\]](#)
- [26] Hebbar, N.; Praveen, B. M.; Prasanna, B. M.; Venkatesha, T. *Trans. Indian Inst. Met.* **2015**, 68, 543. [\[Crossref\]](#)
- [27] Varadharaj, V.; Ramaswamy, A.; Sakthivel, R.; Subbaiya, R.; Barabadi, H.; Chandrasekaran, M.; Saravanan, M. *J. Clust. Sci.* **2020**, 31, 1257. [\[Crossref\]](#)
- [28] Badiger, K. B.; Giddaerappa, R.; Hanumanthappa, L. K.; Sannegowda, K. *Chemistry Select.* **2022**, 7, e202104033. [\[Crossref\]](#)
- [29] Hanumegowda, S.; Srinivasa, C.; Shivaiah, A.; Venkatappa, M.; Hanumanthappa, R.; Rangappa, R.; Laxmaiah, R.; Gonchigar, S.; Sannanigaiah, D. *Asian Pac. J. Trop. Biomed.* **2022**, 12, 47. [\[Crossref\]](#)
- [30] Khan, M.; Sohail, N. I.; Raja, M. J.; Asad, Z.; Mashwani, R. *Sci. Rep.* **2023**, 13, 4514. [\[Crossref\]](#)
- [31] Hebbar, N.; Mokshanatha, P. B.; Bennehalli Mathad, P.; Venkatesha, T. V. *Mor. J. Chem.* **2015**, 3, 496. [\[Crossref\]](#)

- [32] Praveen, B. M.; Prasanna, B. M.; Hebbar, N.; Kumar, P. S.; Jagadeesh, B. M. *J. Bio- Tribo-Corros.* **2018**, 4, 21. [\[Crossref\]](#)
- [33] Hebbar, N.; Praveen, B. M.; Prasanna, B. M.; Vishwanath, P. *J. Fail. Anal. Prev.* **2020**, 20, 1516. [\[Crossref\]](#)

How to cite this article

Pruthviraj K.; Chethan, B. S.; Ramesha H.; Lokanath N. K.; Kiran P. C.; Devaraju K. S.; Hebbar N.; Sunil. K. *Orbital: Electron. J. Chem.* **2024**, 16, 198. DOI: <http://dx.doi.org/10.17807/orbital.v16i3.21006>